Pakistan Veterinary Journal

ISSN: 0253-8318 (PRINT), 2074-7764 (ONLINE)
DOI: 10.29261/pakvetj/2026.188

RESEARCH ARTICLE

Quercetin Ameliorates Tunicamycin-Induced Hepatic Endoplasmic Reticulum Stress and Steatosis Involving the G Protein-Coupled Estrogen Receptor Pathway in Rabbits

Yao Yao[1,2], Le Shao[1,2], Pin Zhai[1,2], Jie Yang[1,2], Jian Li[1,2], Xia Zhang[1,2] and Feng Qin[1,2]*

[1]Institute of Animal Science, Jiangsu Academy of Agricultural Sciences, Nanjing, 210014, China; [2] Key Laboratory of Crop and Livestock Integrated Farming, Ministry of Agriculture, Nanjing, 210014, China.
*Corresponding author: 1486611290@qq.com

ARTICLE HISTORY (26-701)

Received: June 7, 2026
Revised: August 16, 2026
Accepted: August 20, 2026
Published online: August 22, 2026

Key words:
Antioxidant
Endoplasmic reticulum stress
Hepatic steatosis
Quercetin
Rabbit

ABSTRACT

This study evaluated the effects of the natural flavonoid quercetin (QUE) in regulating liver endoplasmic reticulum (ER) stress and hepatic fat accumulation in tunicamycin (TM)-induced rabbits and explored the underlying molecular mechanisms. New Zealand rabbits (n = 96) were subjected to random assignment into four groups, including normal control (NC), QUE-treated (QUE), TM-challenged (TM), and TM-challenged with QUE (TM+QUE). Our findings demonstrate that QUE treatment significantly ameliorated hepatic histopathological steatosis and relieved liver damage in TM-induced rabbits. QUE improved lipid parameters and ameliorated TM-induced hepatic lipid metabolism disorders. Importantly, QUE attenuated TM-induced hepatic ER stress and oxidative damage in TM-induced rabbits. Meanwhile, QUE suppressed excessive proinflammatory cytokine production and restrained the nuclear factor κB (NF-κB) signaling activation in TM-induced rabbits. Furthermore, QUE increased phosphorylation level of AMP-activated protein kinase (AMPK) and enhanced the protein abundance of G protein-coupled estrogen receptor (GPER). Overall, these results reveal that QUE mitigates hepatic steatosis and ER stress involving the GPER/AMPK pathway, thereby alleviating oxidative stress and inflammatory injury, which supports its potential as a promising nutraceutical for preventing hepatic diseases in rabbits.

To Cite This Article: Yao Y, Shao L, Zhai P, Yang J, Li J, Zhang X and Qin F, 2026. Quercetin ameliorates tunicamycin-induced hepatic endoplasmic reticulum stress and steatosis involving the g protein-coupled estrogen receptor pathway in rabbits. Pak Vet J, 46(8): 2118-2127. http://dx.doi.org/10.29261/pakvetj/2026.188

INTRODUCTION

The liver serves as the central organ in maintaining systemic metabolic homeostasis, and exerts a crucial action in coordinating lipid metabolism. Disturbances in fat metabolism evoke various metabolic diseases and threaten the health of humans and animals. Metabolic dysfunction-associated steatotic liver disease (MASLD) is pathologically featured by abnormal buildup of lipids within hepatocytes (Miao *et al*., 2024). MASLD development arises from a complex interplay of multiple pathogenic factors, with the "multiple-hit" hypothesis emerging as a central mechanism. Hepatic steatosis (the "first hit") is exacerbated by parallel insults, such as oxidative stress and inflammation, thereby propelling disease progression (Li *et al*., 2024). Recent research has identified endoplasmic reticulum (ER) dysfunction as a critical part in the process of MASLD (Venkatesan *et al*., 2023). ER is a vital site of lipid synthesis, and ER stress is considered a key bridge linking lipid overload and hepatic injury (Ajoolabady *et al*., 2023). Nutraceuticals and dietary supplements have emerged as promising adjuncts to prevent the occurrence of MASLD (Vrentzos *et al*., 2025).

Naturally occurring as a polyphenolic flavonoid, quercetin (QUE) is abundant in various edible fruits, vegetables, and grains (Andres *et al*., 2018). QUE exerts lipid-lowering, antioxidant, anti-inflammatory and other biological properties, and serves as a nutraceutical for the regulation of metabolic syndromes (Hosseini *et al*., 2021). QUE has been reported to alleviate fatty liver by normalizing lipid profiles and attenuating oxidative injury (Yang *et al*., 2019). QUE mitigates excessive high-fat diet (HFD)-caused fat deposition in mice (Porras *et al*., 2017). Furthermore, QUE also serves as a critical modulator of ER homeostasis (Eisvand *et al*., 2022). Research has shown that QUE mitigates thapsigargin-induced ER stress in rat hepatocytes (Tang *et al*., 2016). However, whether

QUE ameliorates hepatic steatosis by regulating ER stress remains unclear. Moreover, given that the rabbit's lipoprotein profile more closely resembles that of humans, and its heightened susceptibility to hyperlipidemia than rodents, rabbits are widely utilized as a model for MASLD research.

Hence, the research sought to decode QUE's actions against tunicamycin (TM)-driven steatosis, ER stress, and oxidative stress in New Zealand rabbits. The outcomes established that QUE protects against liver injury and steatosis. Notably, QUE blocks the increase of ER stress-related factors and improves the unfolded protein response (UPR) in TM-induced rabbits. Furthermore, QUE markedly attenuates oxidative stress and inflammation in TM-induced rabbits. The present data furnish QUE's hepatoprotective effects and validate its application against metabolic diseases.

MATERIALS AND METHODS

Experimental design: The experimental protocol was conducted under the ethical oversight of the Jiangsu Academy of Agricultural Sciences (No. 63, July 8, 2014). Ninety-six male weaned rabbits (New Zealand, 28 day old) were randomly allocated to four groups, with eight pens per group and three rabbits per pen. Rabbits were fed the basal diet with or without 400 mg/kg QUE for 20 days. QUE was added directly to the basal diet as a powder. At day 20, rabbits in the TM and TM+QUE groups received a intraperitoneal injection of TM (0.2 mg/kg; Macklin, China); rabbits in the normal control (NC) and QUE groups received DMSO as the control. All injections were performed 1 day before euthanasia, a time interval selected based on previous studies (Chen *et al*., 2020; Yamamoto *et al*., 2010). One rabbit was randomly selected from each pen (n = 8 per group). Blood samples were collected from the rabbit marginal ear vein for serum separation, and liver tissues were harvested for further analysis. The detailed formula of basal feed is shown in Table 1.

Table 1: Composition and nutrient levels of the experimental diets (air-dry basis).

Ingredients (g/kg)		Nutrient levels (%)	
Chrysanthemum powder	380	Digestible energy (MJ/kg)[2]	10.17
Soybean meal	108	CP	16.19
Wheat bran	209	CF	11.57
Corn	220	Crude fat	3.65
NaCl	3	Calcium	1.54
Rapeseed meal	30	Effective phosphorus	0.40
Premix[1]	50	Lysine	0.96
		Arginine	0.82
Total	1000	Methionine + Cysteine	0.47

[1] The detailed composition per kilogram of premix was as follows: 5320 mg $FeSO_4 \cdot H_2O$, 1080 mg $CuSO_4 \cdot 5H_2O$, 560 mg $MnSO_4 \cdot H_2O$, 3652 mg $ZnSO_4 \cdot H_2O$, 1000 mg $CoCl_2 \cdot 6H_2O$, 180,000 IU VA, 18,000 IU VD, 900,000 IU VE, 250 g $CaHPO_4$, 60 g lysine, and 40 g methionine. [2] Digestible energy was estimated through total energy, whereas the other indices were assayed directly.

Histopathological analysis: Hepatic tissue samples underwent fixation with 4% paraformaldehyde prior to paraffin embedding, which was conducted in compliance with standard procedures for hematoxylin-eosin (H&E) staining. For hepatic lipid staining via the Oil Red O method freshly isolated tissues were immediately frozen in optimal cutting temperature medium. After cryosection preparation, tissue slices received fixation treatment and Oil Red O staining, and hematoxylin was utilized as the counterstain. Sections were examined under microscope (Olympus, Japan). Blinded histopathological assessments were done by an independent experimenter.

Measurement of biochemical and antioxidant parameters: Serum biochemical and antioxidant parameters were assessed using kits (Jiancheng, China). Hepatic levels of these indicators were standardized against the protein content measured via BCA assay (Beyotime, China). Quantitative detection of serum VLDL, TNF-α, and IL-6 was performed with ELISA kits (Hengyuan, China).

qRT-PCR analysis: Total RNA extraction was performed with TRIzol, and subsequent cDNA synthesis was completed using commercial kits (Vazyme, China). Then, qRT-PCR was conducted and target gene was standardized relative to β-actin and quantified by the $2^{-\Delta\Delta CT}$ method. Specifically, four biological replicates and two technical replicates per biological sample were performed. The primers are detailed in Table 2, and all primers were synthesized by TsingKe Biotechnology (Beijing, China).

Table 2: Primer sequences of targeted genes and β-actin.

Gene	GenBank accession number	Primer sequences (5'-3')	Product size (bp)
β-actin	NM_001101683	F: TTCCAGCCCTCCTTCCT R: GTCCACGTCGCACTTCA	81
PPARα	XM_070053050	F: TGGAGACCGTCACAGA R: CCATTCCCGTAGGC	169
CPT1	XM_051827875	F: ATTCTCACCGCTTTGGGAGG R: ACGGGGTTTTCTAGGAGCAC	196
APOB	XM_008254783	F: TGGCTGCCTATCTC R: CACCTGCTCATTCC	92
SREBP-1c	XM_051829023	F: CGCCATCCACCATAACC R: GGAGTCCATTGCCTACCC	110
GRP78	XM_051836812	F: GGTGGAACCTTTGAT R: TTGCCAGTCTTCTTTT	149
CHOP	XM_070052518	F: AAGCCACCAGCACCTC R: CACTCTGTTTCCGTTTCC	111
GADD34	XM_051828805	F: CTGCGAAGGCGGCTCAA R: TCCCTGGCGAACTGCT	170
TNF-α	NM_001082263	F: GTATGATCCGGGACG R: CACGAGCAGGAAAGAG	110
COX-2	NM_001082388	F: TTTGCTGAAGCCCTAT R: CATCAATGTCGCCGTA	89
iNOS	XM_017349096	F: GAGGTGGGCAGGAGGAT R: GGAGCACGGCGATGTT	91
Nrf2	XM_051849403	F: GCCTCCACCTCCTTA R: ATACATTGCCGTCCC	129
Keap1	XM_008251550	F: CGACCCAGACACTGACACC R: CCCTGCCTAAGGAACACG	142
SOD2	XM_051854201	F: AGGGTTCAGGATGGG R: GCAGGTAGTAAGCGTGTT	147
HO-1	XM_070051491	F: TTTAAGCTGGTGATGGC R: CTCCTCCGGGAAGTAGA	108
IL-6	NM_001082064	F: TGGCGGAAGTCAATCT R: CAGCAGGCAGGTCTCA	86

Abbreviations: PPARα, peroxisome proliferator-activated receptor α; CPT1, carnitine palmitoyl transferase 1; APOB, apolipoprotein B; SREBP-1c, sterol regulatory element binding protein-1c; GRP78, glucose-regulated protein 78; CHOP, C/EBP-homologous protein; GADD34, growth arrest and DNA damage-inducible 34; Nrf2, nuclear factor (erythroid-derived 2)-like 2; Keap1, Kelch-like ECH-associated protein 1; SOD2, superoxide dismutase 2; HO-1, heme oxygenase-1; iNOS, inducible nitric oxide synthase; COX-2, cyclooxygenase-2; TNF-α, tumor necrosis factor-α; IL-6, interleukin 6.

Western blotting: Liver lysates were prepared in lysis buffer for protein assays. Proteins samples were separated by SDS-PAGE, blotted onto PVDF membranes, and blocked. After primary antibody binding overnight, blots were reacted with HRP-conjugated secondary antibodies. Band visualization was achieved with ECL reagents, and quantification was performed using ImageJ. Blinded Western blots were done by an independent experimenter.

Molecular docking: The grid box was centered at the coordinates (109.567, 120.909, 108.311) Å, which are located within the active domain of the target protein. A total of 112, 120 and 150 grid points were assigned along the X, Y, and Z axes, respectively, with a grid spacing of 0.4861 Å. The resulting box dimensions were 54.44 × 58.33 × 72.92 Å, fully enclosing the ligand-binding cavity. The 3D structure of G-protein coupled estrogen receptor (GPER) was retrieved from the RCSB Protein Data Bank, and that of QUE from PubChem. The protein structure was dehydrated and hydrogenated using PyMOL. Molecular docking of GPER with QUE was then performed using AutoDock. Docking poses were visualized and analyzed in PyMOL.

Statistical analysis: Data are presented as mean±SEM. Statistical comparisons among groups were performed using ANOVA with IBM SPSS 20.0 (IBM Corp., Chicago, IL, USA), followed by LSD post hoc test for pairwise multiple comparisons. A value of $P < 0.05$ was considered statistically significant.

RESULTS

QUE mitigates hepatic histopathological steatosis and relieves hepatic damage in TM-induced rabbits: The H&E staining illustrated that TM treatment evoked architectural distortion of the hepatic cords and vacuolar degeneration of hepatocytes. However, QUE supplementation effectively attenuated the TM-induced micro-vesicular steatosis (Fig. 1A). Furthermore, QUE treatment significantly ameliorated the excessive hepatic lipid droplet deposition induced by TM (Fig. 1B). In addition, QUE treatment obviously increased serum TP and ALB contents while lowering AST and ALT levels in TM-challenged rabbits (Fig. 1C-F).

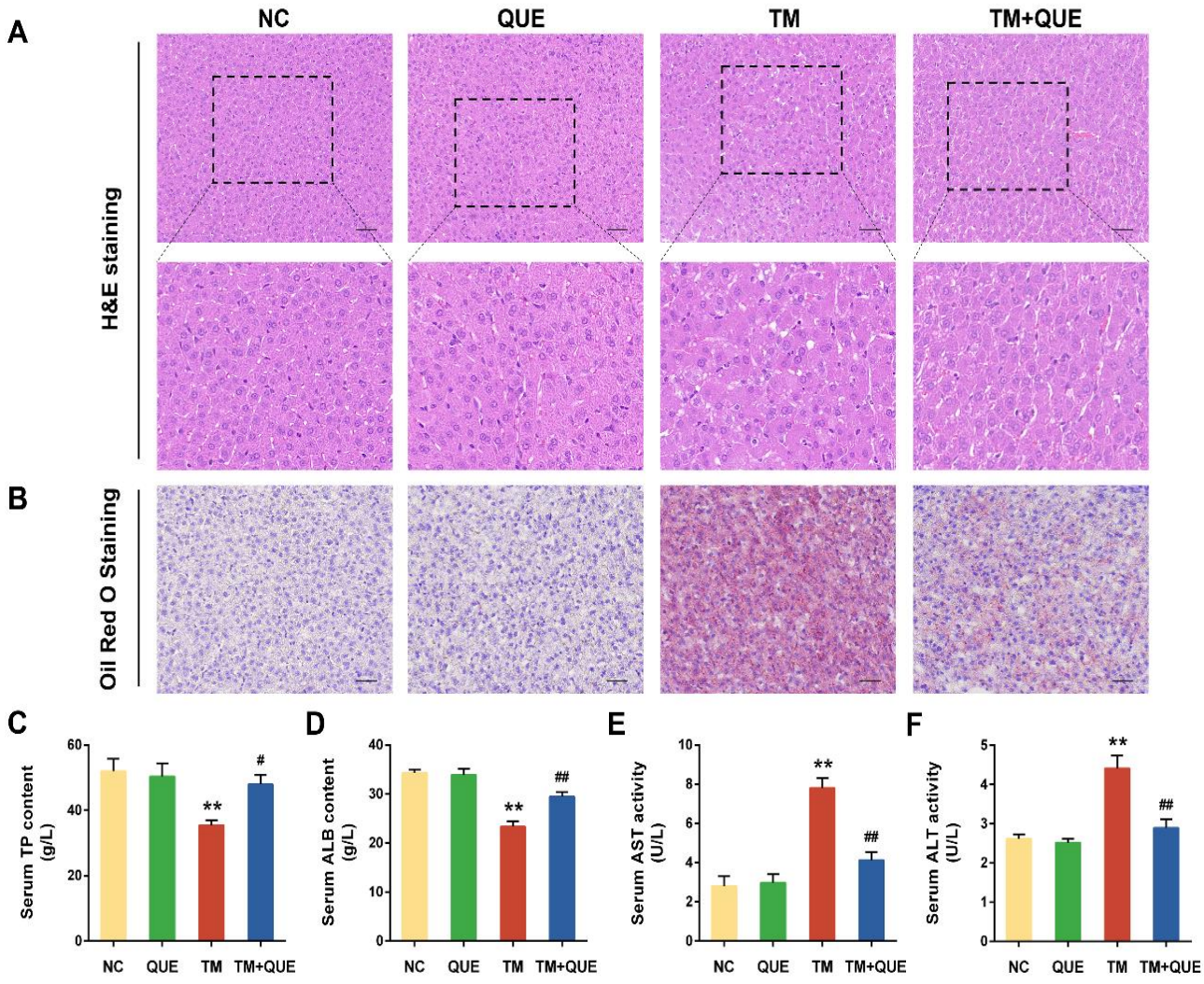

Fig. 1: Impacts of QUE on hepatic pathological observation and function of rabbits induced by TM. (A) H&E staining of liver sections. Scale bars: 50 μm. (B) Oil Red O staining of liver sections. Scale bars: 50 μm. (C–F) Serum biochemical parameters including total protein (TP; C), albumin (ALB; D), AST (E), and ALT (F), respectively. Values are given as means ± SEM. Significant differences versus the NC group are indicated by **P<0.01, and versus the TM group by #P<0.05 and ##P<0.01.

QUE improves lipid parameters and ameliorates hepatic lipid metabolism disorders in TM-induced rabbits: As shown in Fig. 2A-E, TM depressed serum contents of TC, TG, LDL-C, HDL-C, and VLDL versus NC group, whereas QUE treatment markedly elevated these lipid parameters in comparison to TM group. Moreover, the TM-stimulated accumulation of hepatic TG and TC was effectively inhibited by QUE supplementation in rabbits (Fig. 2F and G). As displayed in Fig. 3A-D, compared with NC group, TM treatment significantly downregulated the transcript abundance of *APOB* (fatty acid transporter) and lipolysis-related factor, such as *PPARα* and *CPT1*, while upregulated the mRNA expression of lipogenic factor *SREBP-1c*. However, QUE supplementation enhanced the mRNA expression of *PPARα*, *CPT1* and *APOB* and inhibited *SREBP-1c* mRNA expression in the liver of rabbits triggered by TM (Fig. 3A-D). Concurrently, QUE treatment effectively reversed the decrease in ACCα protein phosphorylation in the liver of rabbits induced by TM (Fig. 3E-F).

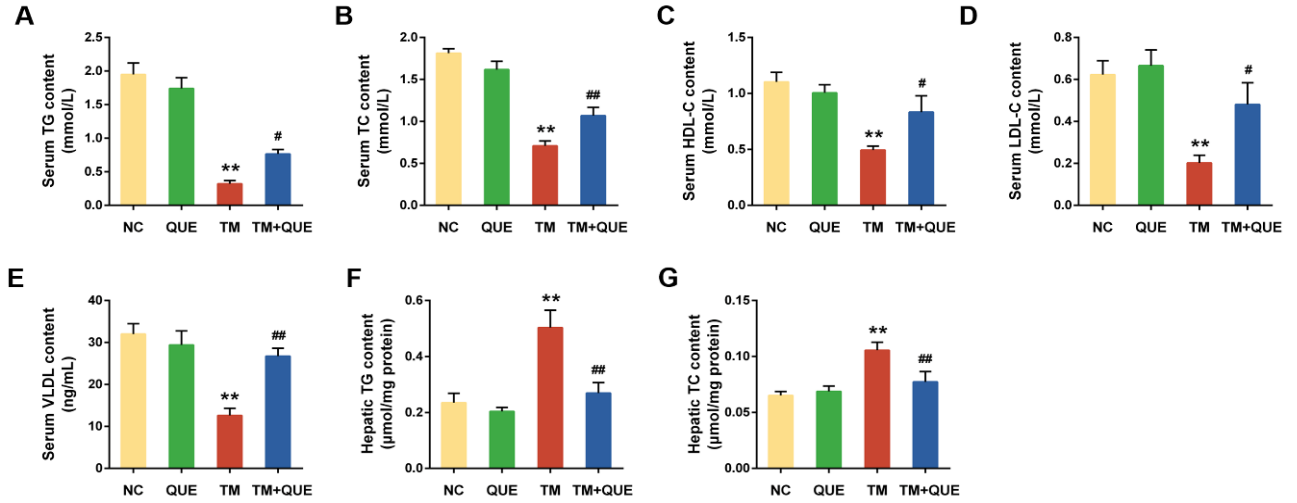

Fig. 2: Impacts of QUE on serum and hepatic lipid parameters in TM-induced rabbits. (A–E) Serum concentrations of triglyceride (TG; A), total cholesterol (TC; B), high-density lipoprotein cholesterol (HDL-C; C), low-density lipoprotein cholesterol (LDL-C; D), and very low-density lipoprotein (VLDL; E), respectively. (F, G) Hepatic TG (F) and TC (G) contents, respectively. Values are given as means ± SEM. Significant differences versus the NC group are indicated by **P<0.01, and versus the TM group by #P<0.05 and ##P<0.01.

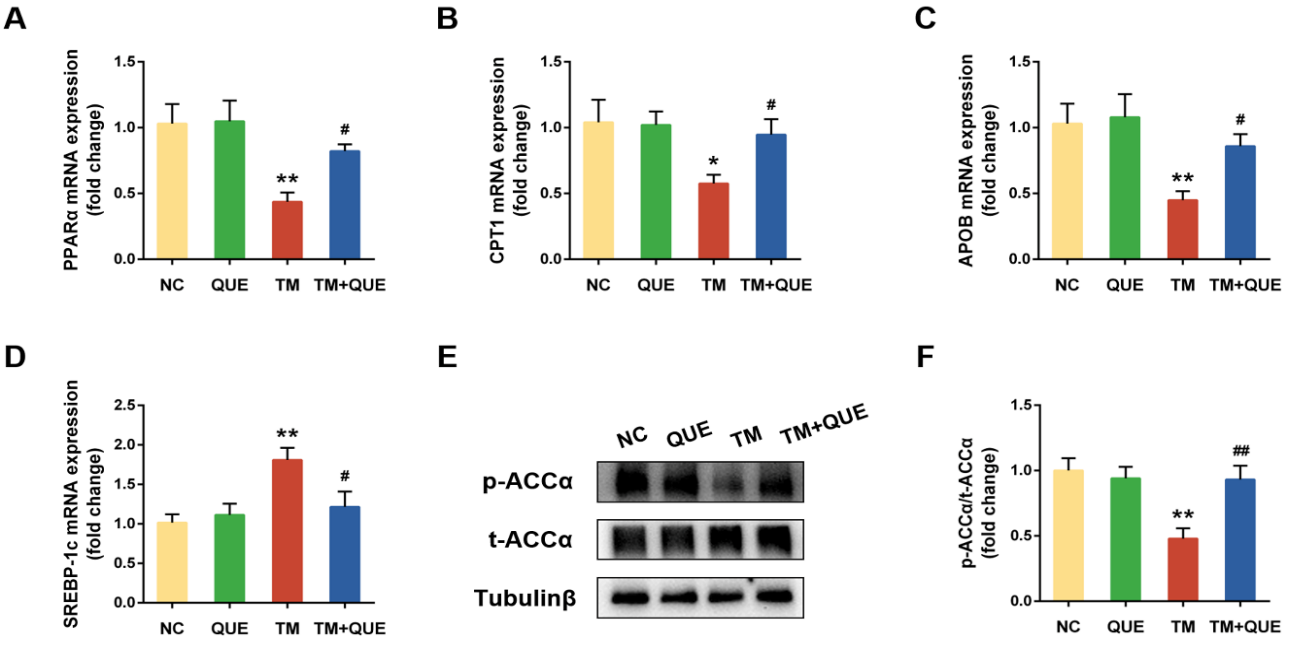

Fig. 3: Impacts of QUE on the abundance of hepatic lipid metabolism-related factors in TM-induced rabbits. (A–D) qRT-PCR analysis of the mRNA transcript levels of peroxisome proliferation activated receptor α (PPARα; A), carnitine palmitoyl transferase I (CPT1; B), apolipoprotein B (APOB; C), sterol regulatory element binding protein-1c (SREBP-1c; D), respectively. (E–F) Immunoblotting results for total and phosphorylated ACCα (E), along with the corresponding p-ACCα/t-ACCα ratio (F). Values are given as means±SEM. Significant differences versus the NC group are indicated by *P<0.05 and **P<0.01, and versus the TM group by #P<0.05 and ##P<0.01.

QUE attenuates TM-induced hepatic ER stress and improves UPR in rabbits: As displayed in Fig. 4A-C, compared with NC group, TM markedly elevated ER stress-linked factors *GRP78*, *CHOP* and *GADD34* mRNA abundance. Meanwhile, the expression of UPR related proteins, including phosphorylated IRE1α, phosphorylated PERK and ATF6, as well as GRP78 and CHOP were significantly promoted by TM stimulation in liver of

rabbits (Fig. 4D-I). Notably, QUE intervention counteracted the overexpression of ER stress factors and attenuated UPR in TM-induced rabbits (Fig. 4).

QUE enhances antioxidant capacity and improves oxidative stress in TM-induced rabbits: TM treatment showed higher serum or hepatic MDA and H_2O_2 contents but lower T-AOC, CAT, POD, and T-SOD activities versus the NC group, QUE supplementation decreased MDA and H_2O_2 content, while enhanced antioxidant capacity (Fig. 5). Compared with the NC group, TM dampened antioxidant gene abundance (*Nrf2*, *SOD2* and *HO-1*) and enhanced *Keap1* level, whereas QUE reversed these alterations in TM-challenged rabbits (Fig. 6A-D). Meanwhile, QUE enhanced hepatic Nrf2 and its downstream target protein HO-1 and NQO1 levels (Fig. 6E-H).

QUE suppresses the overproduction of proinflammatory cytokines and blocks NF-κB signaling in TM-challenged rabbits: As illustrated in Fig. 7A and B, the TM-caused enhancement of serum TNF-α and IL-6 concentrations were suppressed by QUE. QUE supplementation effectively inhibited the overproduction of proinflammatory mediators (TNF-α, iNOS, IL-6, and COX-2) in comparison to the TM group (Fig. 7C-F). Moreover, QUE supplementation significantly suppressed the phosphorylation of IκBα and NF-κBα p65 proteins (Fig. 7G-I).

QUE activates the GPER/AMPK pathway in TM-induced rabbits: As shown in Fig. 8A and B, hepatic AMPKα phosphorylation was attenuated in TM-induced rabbits compared with NC group, whereas QUE treatment significantly reversed the decrease. In addition, QUE markedly upregulated the protein expression of GPER in liver of rabbits treated with TM (Fig. 8A and C). Molecular docking analysis showed that QUE effectively bound to the ligand-binding domain of GPER (Fig. 8D and E).

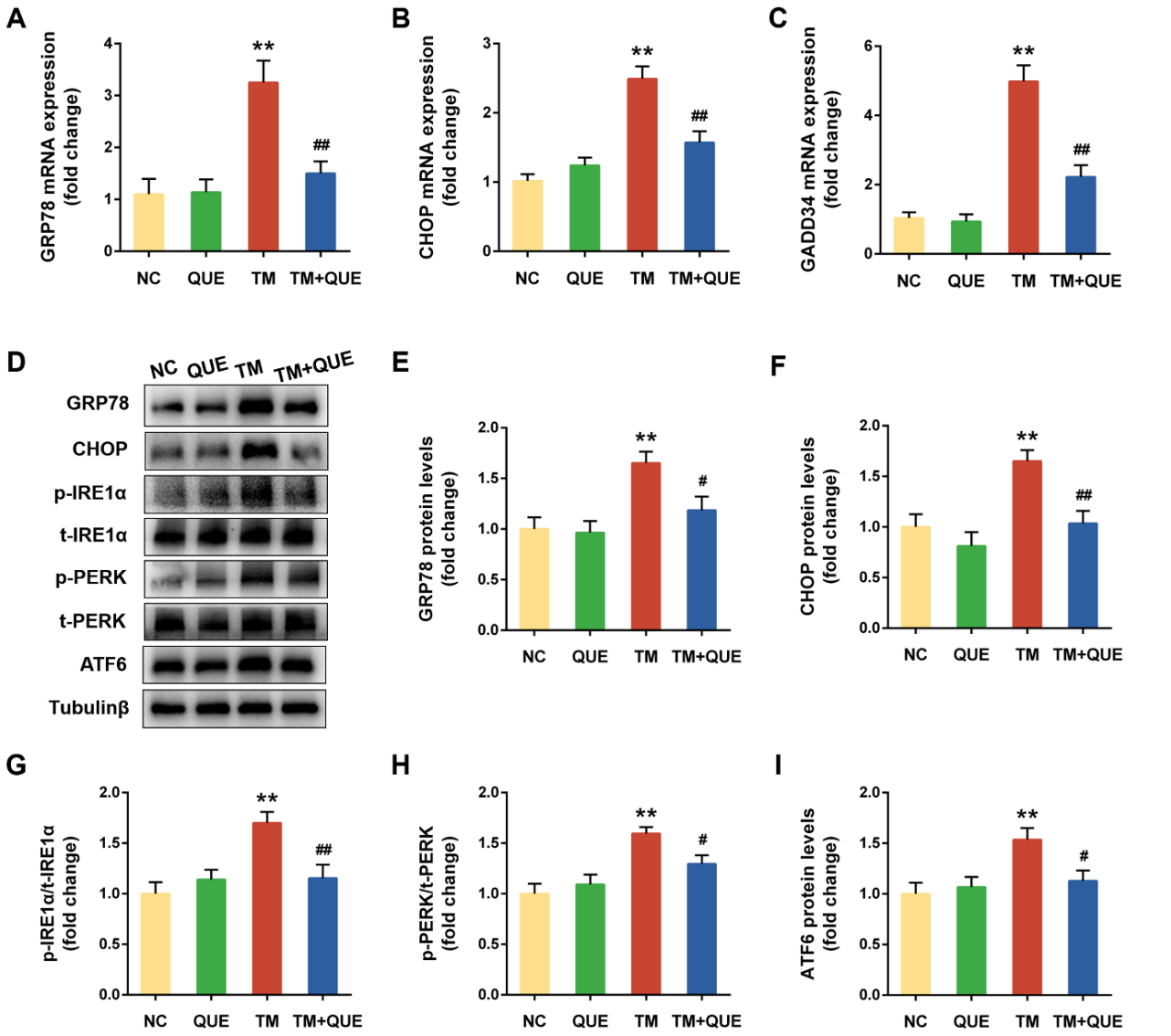

Fig. 4: Impacts of QUE on TM-induced ER stress and unfolded protein response in rabbit liver. (A–C) qRT-PCR analysis of the mRNA transcript levels of glucose-regulated protein 78 (GRP78; A), C/EBP-homologous protein (CHOP; B), growth arrest and DNA damage-inducible 34 (GADD34; C), respectively. (D–G) Immunoblotting results for total or phosphorylated GRP78, CHOP, IRE1α, PERK, and ATF6 (D), with the corresponding quantitative results of GRP78 (E), CHOP (F), p-IRE1α/t-IRE1α ratio (G), p-PERK/t-PERK (H), ATF6 (I), respectively. Values are given as means±SEM. Significant differences versus the NC group are indicated by $^{**}P<0.01$, and versus the TM group by $^{\#}P<0.05$ and $^{\#\#}P<0.01$.

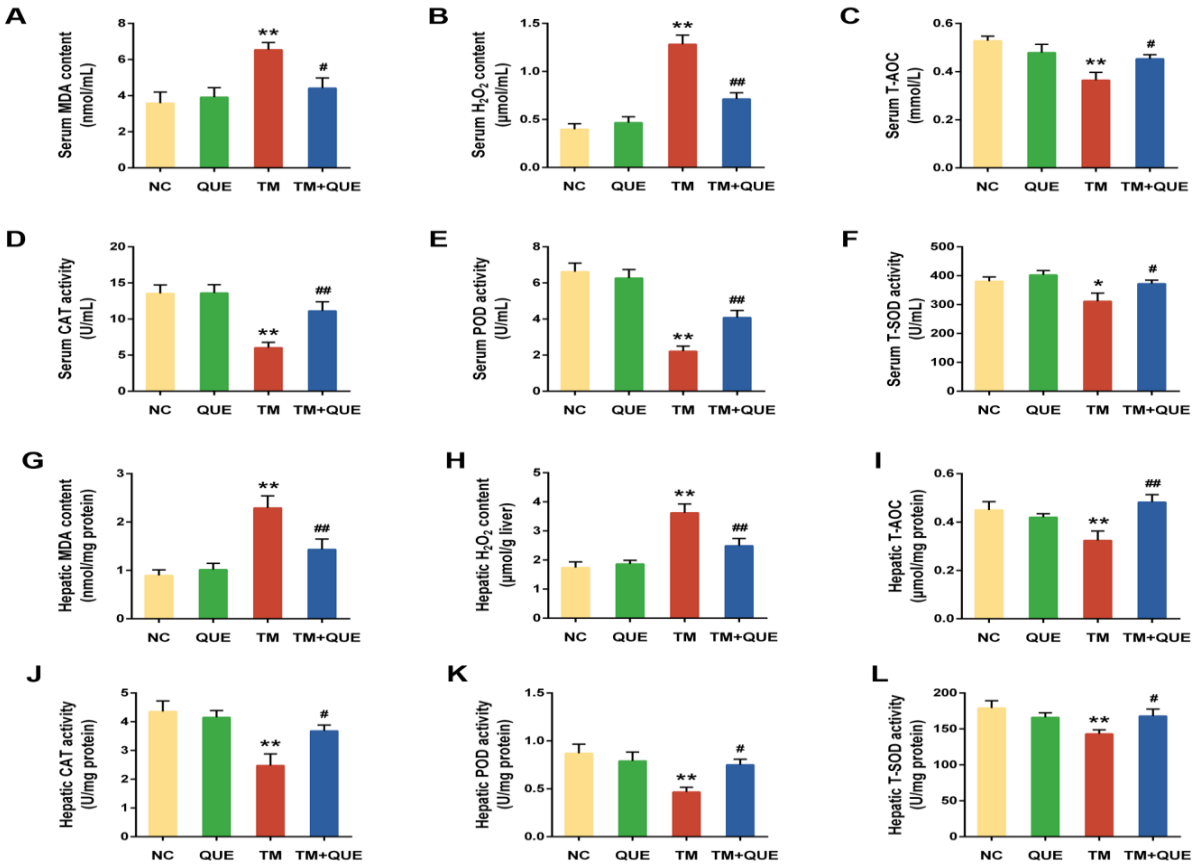

Fig. 5: Impacts of QUE on oxidative stress markers and antioxidant capacit in the serum and liver of TM-induced rabbits. (A–F) Serum levels of malondialdehyde (MDA; A), hydrogen peroxide (H_2O_2; B), total antioxidant capacity (T-AOC; C), catalase (CAT; D), peroxidase (POD; E), total superoxide dismutase (T-SOD; F), respectively. (G–L) Corresponding parameters in hepatic tissues. Values are given as means±SEM. Significant differences versus the NC group are indicated by *P<0.05 and **P<0.01, and versus the TM group by $^{\#}$P<0.05 and $^{\#\#}$P<0.01.

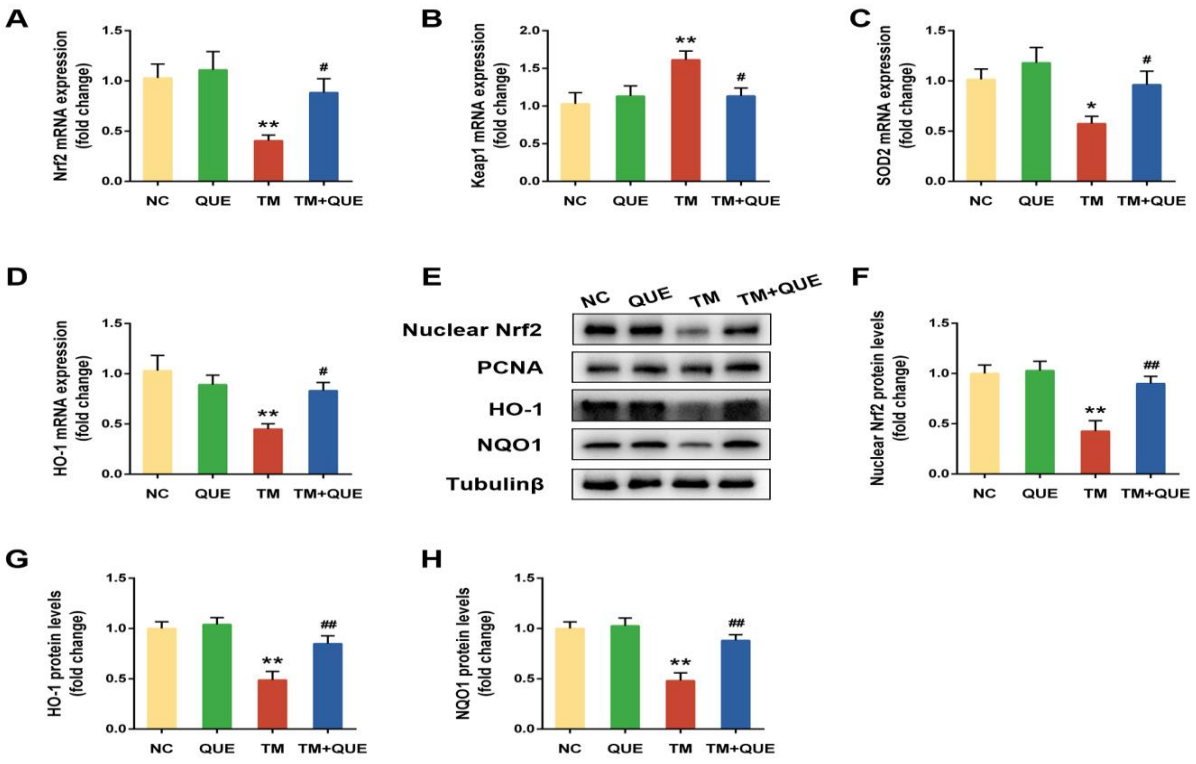

Fig. 6: Impacts of QUE on hepatic oxidative stress-related transcriptional and Nrf2 signaling responses in TM-induced rabbits. (A–D) qRT-PCR analysis of the mRNA transcript levels of nuclear factor (erythroid-derived 2)-like 2 (Nrf2; A), kelch-like ECH-associated protein 1 (Keap1; B), superoxide dismutase 2 (SOD2; C), heme oxygenase-1 (HO-1; D), respectively. (E–H) Immunoblotting results for nuclear Nrf2, HO-1 and NADPH Quinone acceptor Oxidoreductase 1 (NQO1) (E), with the corresponding quantitative results of nuclear Nrf2 (F), HO-1 (G), NQO1 (H), respectively. Values are given as means±SEM. Significant differences versus the NC group are indicated by *P<0.05 and **P<0.01, and versus the TM group by $^{\#}$P<0.05 and $^{\#\#}$P<0.01.

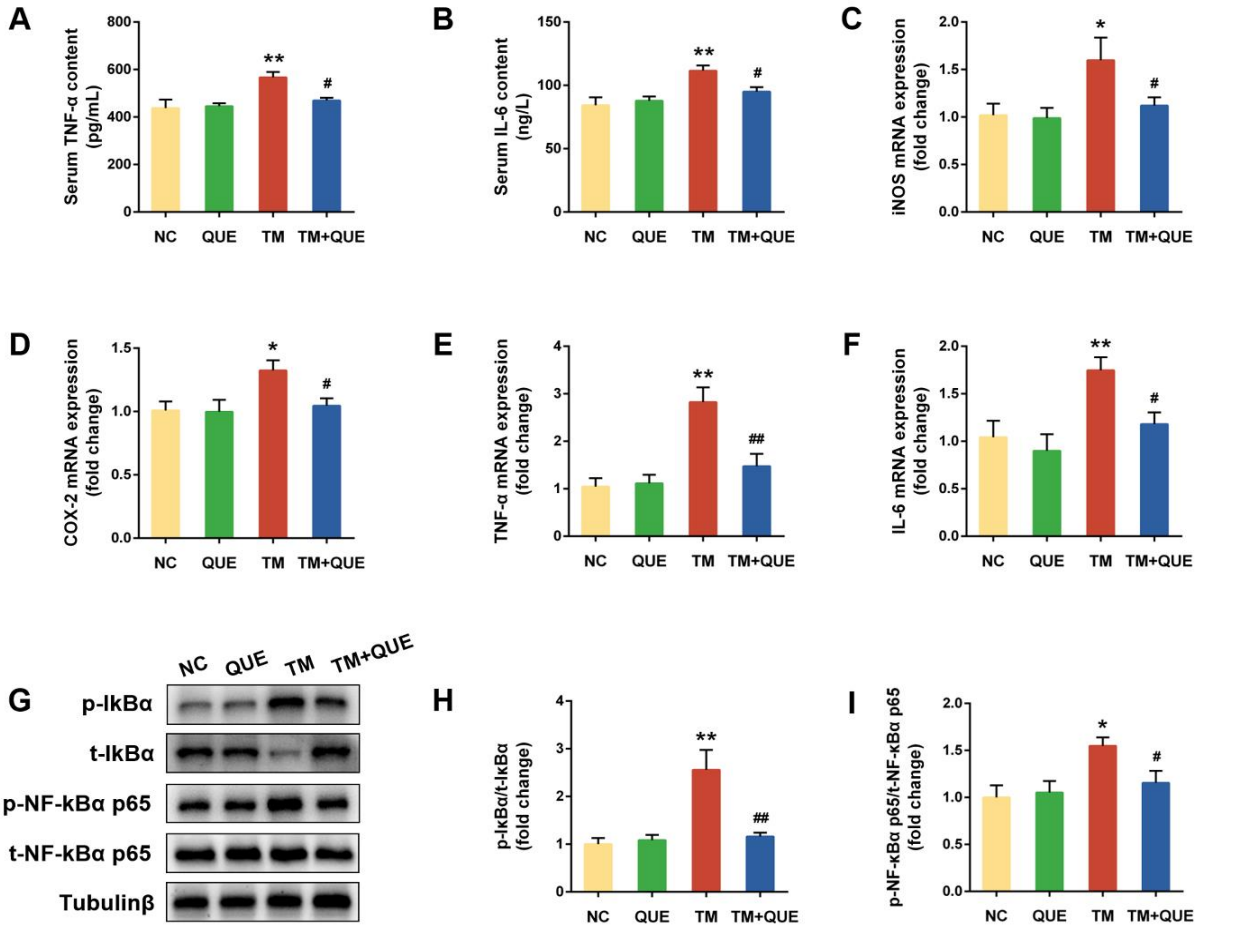

Fig. 7: Impacts of QUE on serum proinflammatory cytokines and hepatic expression of inflammation-related mediators in TM-induced rabbits. (A, B) Serum levels of tumor necrosis factor α (TNF-α; A) and interleukin-6 (IL-6; B). (C–F) qRT-PCR analysis of the mRNA transcript levels of inducible nitric oxide synthase (iNOS; C), cyclooxygenase-2 (COX-2; D), tumor necrosis factor α (TNF-α; E), interleukin-6 (IL-6; F), respectively. (G–I) Immunoblotting results for total (t)-IκBα, phospho (p)-IκBα, t-NF-κBα p65, and p-NF-κBα p65 (G), with the corresponding quantitative results of p-IκBα/t-IκBα (H) and p-NF-κBα p65/t-NF-κBα p65 (I), respectively. Values are given as means±SEM. Significant differences versus the NC group are indicated by *P<0.05 and **P<0.01, and versus the TM group by #P<0.05 and ##P<0.01.

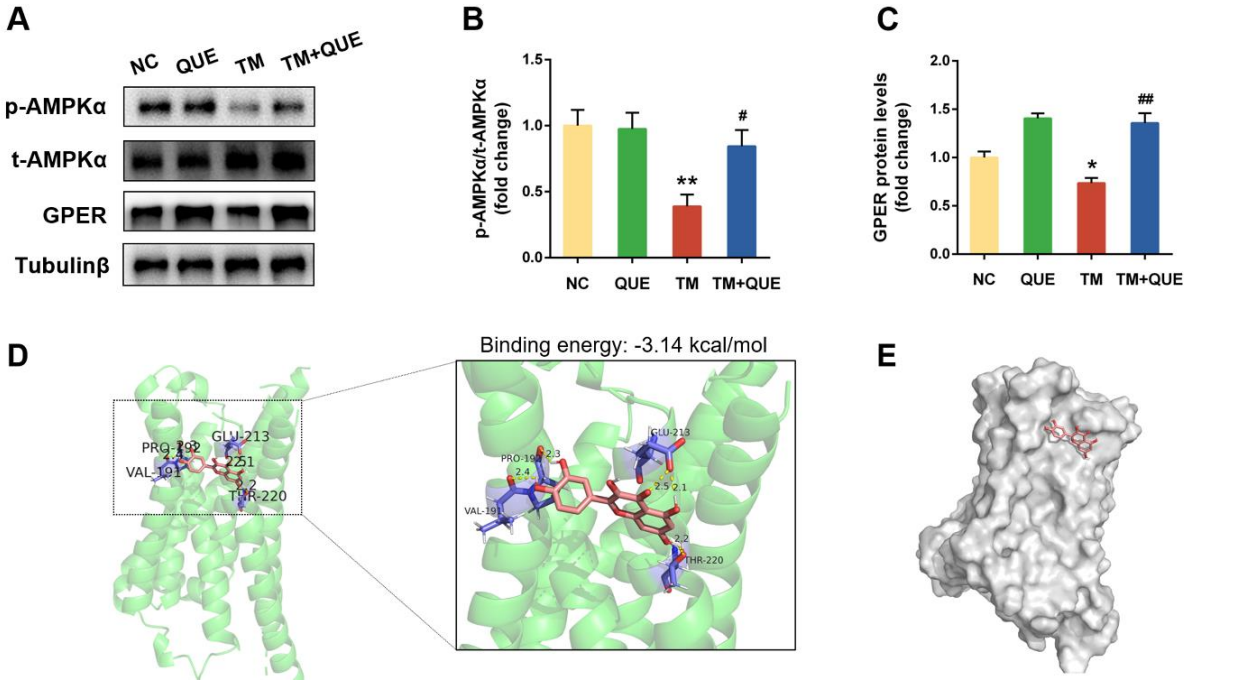

Fig. 8: Impacts of QUE on the GPER-AMPK pathway. (A–C) Immunoblotting results for total (t)-AMPKα, phospho (p)-AMPKα, and G protein-coupled estrogen receptor (GPER) (A), with the corresponding quantitative results of p-AMPKα/t-AMPKα (B) and GPER (C), respectively. (D) Molecular docking results of QUE and GPER; E: Molecular docking results of QUE and protein-binding pocket. Values are given as means±SEM. Significant differences versus the NC group are indicated by *P<0.05 and **P<0.01, and versus the TM group by #P<0.05 and ##P<0.01.

DISCUSSION

Hepatic steatosis is marked by abnormal lipid buildup within cytoplasm (Loomba *et al*., 2021). As a vital site of lipid synthesis, ER exerts a critical role in maintaining lipid homeostasis in hepatocytes. TM, a well-established pharmacological inducer of ER stress, is frequently employed to establish a MASLD model in mice (Feng *et al*., 2017). Presently, QUE significantly relieved TM-induced hepatic histopathological abnormalities and hepatic steatosis. ALT and AST are enzymes localized within the hepatocyte cytoplasm under physiological conditions, while they are released into bloodstream when hepatocellular damage occurs (Zou *et al*., 2020). Moreover, TP and ALB are fundamental biochemical markers reflective of hepatic synthetic function (Matoori *et al*., 2019). In current research, QUE supplementation attenuated ALT and AST activities, while increased TP and ALB contents, which implied that QUE effectively improved TM-induced hepatic damage in rabbits.

ER integrity is essential for systemic lipid homeostasis, and its dysfunction promotes the progression of multiple metabolic diseases including obesity, diabetes mellitus and inflammation. Previous studies found that ER stress-induced lipid accumulation is primarily mediated by enhanced lipogenesis, impaired VLDL secretion, and suppressed fatty acid oxidation (Jo *et al*., 2013). QUE significantly suppressed the excessive hepatic lipid contents induced by TM. Moreover, TM-induced ER stress impaired VLDL secretion and inhibited hepatic lipid efflux, thereby reducing serum lipid levels, which were effectively reversed by QUE supplementation. Overall, these data preliminary implied that QUE improves TM-induced lipid parameters disorders. However, enhanced hepatic lipid uptake, altered bile acid metabolism, or increased peripheral lipid utilization could participate in modulating circulating lipid levels. Future studies are warranted to quantify these parameters and to systematically investigate the potential roles of alternative pathways in the context of TM-induced ER stress and QUE intervention. Excessive intracellular lipid accumulation is driven by the imbalance between lipid acquisition and removal. ER regulates lipid metabolic homeostasis by modulating the expression of key lipid metabolism factors (Chen *et al*., 2016). In this study, QUE restored the TM-downregulated PPARα and CPT1 expression, which promote lipolysis. SREBP-1c regulates lipogenic enzymes such as ACC (Yan *et al*., 2024). QUE improves hepatic lipid metabolism disorders through regulating the expressions of lipid transport, lipogenesis and lipolysis related factor under TM-induced ER stress.

The UPR is a defensive procedure upon ER stress and initiated through three key sensors: IRE1α, PERK, and ATF6 (Hotamisligil, 2010; Hetz *et al*., 2020). GRP78 serves as a binding partner for these sensors, keeping them in a quiescent state during homeostasis. However, misfolded protein overload prompts UPR sensor activation, and the CHOP triggers genotoxic stress and enhances ROS generation (Hetz *et al*., 2020). QUE has been implicated in ER homeostasis in recent research (Eisvand *et al*., 2022). QUE ameliorates ER stress through modulating GRP78 and CHOP expression in TM-induced endothelial cells (Suganya *et al*., 2014); meanwhile, QUE improves cadmium-induced ER stress and oxidative stress by inhibiting PERK/IRE1α/ATF6 signaling pathway in BRL-3A cell (Ding *et al*., 2023). Here, QUE inhibited ER stress-related factors and UPR key factors, suggesting that QUE effectively mitigates ER stress through inhibiting UPR activation.

Excessive deposition of lipids and misfolding of proteins drive the imbalance of the system and subsequently triggers oxidative stress responses. As a major endogenous ROS, H_2O_2 can give rise to highly reactive hydroxyl radicals, leading to oxidative injury to lipids, proteins, and DNA. In general, MDA is widely regarded as a primary biomarker for lipid peroxidation. QUE has been reported to inhibit hypoxia-mediated overproduction of ROS and oxidative stress (Chang *et al*., 2021). Besides, QUE improves oxidative stress and ER stress in rat liver via the IRE1 signal (Liu *et al*., 2013). Furthermore, QUE ameliorates H_2O_2-induced cellular injury by Nrf2 signaling activation (Weng *et al*., 2017). Here, QUE supplementation effectively alleviated hepatic oxidative stress related to the Nrf2 pathway in TM-induced rabbits.

Perturbed intracellular redox homeostasis triggers inflammatory responses, ultimately exacerbating oxidative injury and hepatic damage (Luci *et al.*, 2020). QUE holds promise as a therapy to mitigate inflammatory disorders (Xu *et al.*, 2025). In the study, QUE administration suppressed the transcription and release of pro-inflammatory mediators. Basally, IκBα anchors NF-κB in the cytoplasm, whereas IκBα degrades and NF-κB translates into nucleus when stimulated by inflammatory signals. QUE suppressed ER stress and the subsequent inflammatory response triggered by thapsigargin through inhibiting NF-κB pathway in primary rat hepatocytes (Tang *et al.*, 2016). In this study, QUE mitigates the TM-triggered hepatic inflammatory response through inhibition of NF-κB.

AMPK is well-established as a key modulator of lipid metabolism (Jiang *et al.*, 2025). Studie indicated that AMPK signal improves hepatic steatosis via inhibition of ACC activity and promotion of fatty acid β-oxidation in mice (Yan *et al.*, 2024). Consistently, our previous research found that AMPK activation relieved lipid metabolism disorders in mice (Li *et al.*, 2020). AMPK-mediated suppression of ER stress effectively relieved hepatic lipid deposition (Ahn *et al.*, 2024). Notably, QUE supplementation effectively alleviates fatty liver disease and oxidative stress through activating AMPK signal (Cao *et al.*, 2023). Currently, the suppression of AMPKα caused by TM was restored by QUE, which suggested that QUE alleviates steatosis and ER stress maybe mediated by AMPK signal. QUE, as a flavonoid compound, is similar to estrogen in chemical structure and can effectively bind to estrogen receptors (ERs) (Wilkinson *et al.*, 2015). GPER is widely distributed in various tissues and mediates rapid non-genomic effects of estrogen (Périan and Vanacker, 2020). GPER agonist G1 ameliorates obesity and diabetes in HFD-fed mice and alleviates hepatic steatosis and inflammation via AMPK signaling (Sharma *et al.*, 2020; Li *et al.*, 2021). Here, QUE promoted the expression of GPER protein and molecular docking

analysis further demonstrated that there is a good combination between QUE and GPER. Although the present study demonstrates that QUE ameliorates TM-induced ER stress and hepatic steatosis through a mechanism involving the GPER/AMPK pathway, further pharmacological inhibition studies are required to confirm its obligatory role.

However, we acknowledge that the present study did not examine the protein or mRNA abundance of the classical ERα and ERβ in the liver. This represents a limitation of our current work. Given that QUE shares structural similarity with 17β-estradiol and has been reported to bind to both ERα and ERβ (D'Arrigo G *et al*., 2021), the potential interplay between GPER and classical ERs in mediating the hepatoprotective effects of QUE cannot be excluded. Future studies employing selective ERs antagonists or knockout models are warranted to systematically dissect the relative contributions of these receptor pathways to QUE-induced AMPK activation and ER stress alleviation. Nonetheless, our current findings, together with the molecular docking data, strongly support GPER as a critical mediator of QUE's beneficial effects in this rabbit model.

Conclusions: Overall, our results demonstrate that QUE can ameliorate ER stress-mediated hepatic steatosis, oxidative stress and inflammation, potentially via activating the GPER-AMPK cascade. These findings unveiled the mitigative effects and mechanism of QUE against MASLD in a physiologically relevant rabbit model, and position it as a candidate functional supplement for metabolic disease prevention.

Funding: This research was financially supported by the special fund of the China Agriculture Research System (CARS-43-G-2).

Authors contribution: YY and FQ designed the study; YY, JY and JL contributed methodology; YY and XZ performed software; YY and LS contributed validation; YY, LS and PZ conducted data curation; The original draft of the manuscript was written by YY; All authors revised the manuscript and approved the final draft.

REFERENCES

Ahn SH, Lee YJ, Lim DS, *et al*., 2024. Upadacitinib counteracts hepatic lipid deposition via the repression of JAK1/STAT3 signaling and AMPK/autophagy-mediated suppression of ER stress. Biochemical and Biophysical Research Communications 735:150829.

Ajoolabady A, Kaplowitz N, Lebeaupin C, *et al*., 2023. Endoplasmic reticulum stress in liver diseases. Hepatology 77(2):619-639.

Andres S, Pevny S, Ziegenhagen R, *et al*., 2018. Safety aspects of the use of quercetin as a dietary supplement. Molecular Nutrition and Food Research 62(1):1700447.

Cao P, Wang Y, Zhang C, *et al*., 2023. Quercetin ameliorates nonalcoholic fatty liver disease (NAFLD) via the promotion of AMPK-mediated hepatic mitophagy. Journal of Nutritional Biochemistry 120:109414.

Chang X, Zhang T, Meng Q, *et al*., 2021. Quercetin improves cardiomyocyte vulnerability to hypoxia by regulating SIRT1/TMBIM6-related mitophagy and endoplasmic reticulum stress. Oxidative Medicine and Cellular Longevity 2021:5529913.

Chen XQ, Zhang FF, Gong Q, *et al*., 2016. Hepatic ATF6 increases fatty acid oxidation to attenuate hepatic steatosis in mice through peroxisome proliferator-activated receptor α. Diabetes 65(7):1904-1915.

Chen YN, Zhang H, Chen YP, *et al*., 2020. Resveratrol alleviates endoplasmic reticulum stress-associated hepatic steatosis and injury in mice challenged with tunicamycin. Molecular Nutrition and Food Research 64(14):e2000105.

D'Arrigo G, Gianquinto E, Rossetti G, *et al*., 2021. Binding of androgen- and estrogen-like flavonoids to their cognate (non)nuclear receptors: A comparison by computational prediction. Molecules 26(6):1613.

Ding LL, Zhu HL, Wang K, *et al*., 2023. Quercetin alleviates cadmium-induced BRL-3A cell apoptosis by inhibiting oxidative stress and the PERK/IRE1α/ATF6 signaling pathway. Environmental Science and Pollution Research International 30(60):125790-125805.

Eisvand F, Tajbakhsh A, Seidel V, *et al*., 2022. Quercetin and its role in modulating endoplasmic reticulum stress: A review. Phytotherapy Research 36(1):73-84.

Feng B, Huang XH, Jiang DD, *et al*., 2017. Endoplasmic reticulum stress inducer tunicamycin alters hepatic energy homeostasis in mice. International Journal of Molecular Sciences 18(8):1710.

Hetz C, Zhang KZ and Kaufman RJ, 2020. Mechanisms, regulation and functions of the unfolded protein response. Nature Reviews Molecular Cell Biology 21(8):421-438.

Hosseini A, Razavi BM, Banach M, *et al*., 2021. Quercetin and metabolic syndrome: A review. Phytotherapy Research 35(10):5352-5364.

Hotamisligil GS, 2010. Endoplasmic reticulum stress and the inflammatory basis of metabolic disease. Cell 140(6):900-917.

Jiang F, Li MH, Yao TT, *et al*., 2025. Research progress on AMPK in the pathogenesis and treatment of MASLD. Frontiers in Immunology 16:1558041.

Jo H, Choe SS, Shin KC, *et al*., 2013. Endoplasmic reticulum stress induces hepatic steatosis via increased expression of the hepatic very low-density lipoprotein receptor. Hepatology 57(4):1366-1377.

Li LL, Wang HJ, Yao Y, *et al*., 2021. The sex steroid precursor dehydroepiandrosterone prevents nonalcoholic steatohepatitis by activating the AMPK pathway mediated by GPR30. Redox Biology 48:102187.

Li LL, Yao Y, Zhao JL, *et al*., 2020. Dehydroepiandrosterone protects against hepatic glycolipid metabolic disorder and insulin resistance induced by high fat via activation of AMPK-PGC-1α-NRF-1 and IRS1-AKT-GLUT2 signaling pathways. International Journal of Obesity (London) 44(5):1075-1086.

Li YX, Yang PP, Ye JL, *et al*., 2024. Updated mechanisms of MASLD pathogenesis. Lipids in Health and Disease 23(1):117.

Liu CM, Zheng GH, Ming QL, *et al*., 2013. Protective effect of quercetin on lead-induced oxidative stress and endoplasmic reticulum stress in rat liver via the IRE1/JNK and PI3K/Akt pathway. Free Radical Research 47(3):192-201.

Loomba R, Friedman SL and Shulman GI, 2021. Mechanisms and disease consequences of nonalcoholic fatty liver disease. Cell 184(10):2537-2564.

Luci C, Bourinet M, Leclere PS, *et al*., 2020. Chronic inflammation in non-alcoholic steatohepatitis: Molecular mechanisms and therapeutic strategies. Frontiers in Endocrinology 11:597648.

Matoori S, Froehlich JM, Breitenstein S, *et al*., 2019. Serum albumin, total bilirubin, and patient age are independent confounders of hepatobiliary-phase gadoxetate parenchymal liver enhancement. European Radiology 29(11):5813-5822.

Miao L, Targher G, Byrne CD, *et al*., 2024. Current status and future trends of the global burden of MASLD. Trends in Endocrinology and Metabolism 35(8):697-707.

Périan S and Vanacker JM, 2020. GPER as a receptor for endocrine-disrupting chemicals (EDCs). Frontiers in Endocrinology 11:545.

Porras D, Nistal E, Martínez-Flórez S, *et al*., 2017. Protective effect of quercetin on high-fat diet-induced non-alcoholic fatty liver disease in mice is mediated by modulating intestinal microbiota imbalance and related gut-liver axis activation. Free Radical Biology and Medicine 102:188-202.

Sharma G, Hu CL, Staquicini DI, *et al*., 2020. Preclinical efficacy of the GPER-selective agonist G-1 in mouse models of obesity and diabetes. Science Translational Medicine 12(528):5956.

Suganya N, Bhakkiyalakshmi E, Suriyanarayanan S, *et al*., 2014. Quercetin ameliorates tunicamycin-induced endoplasmic reticulum stress in endothelial cells. Cell Proliferation 47(3):231-240.

Tang YH, Li J, Gao C, *et al*., 2016. Hepatoprotective effect of quercetin on endoplasmic reticulum stress and inflammation after intense exercise in mice through phosphoinositide 3-kinase and nuclear factor-kappa B. Oxidative Medicine and Cellular Longevity 2016:8696587.

Venkatesan N, Doskey LC and Malhi H, 2023. The role of endoplasmic reticulum in lipotoxicity during metabolic dysfunction-associated steatotic liver disease (MASLD) pathogenesis. American Journal of Pathology 193(12):1887-1899.

Vrentzos E, Pavlidis G, Korakas E, *et al*., 2025. Nutraceutical strategies for metabolic dysfunction-associated steatotic liver disease (MASLD): A path to liver health. Nutrients 17(10):1657.

Weng SS, Mao L, Gong YY, *et al*., 2017. Role of quercetin in protecting ARPE-19 cells against H_2O_2-induced injury via nuclear factor erythroid 2 like 2 pathway activation and endoplasmic reticulum stress inhibition. Molecular Medicine Reports 16(3):3461-3468.

Wilkinson AS, Taing MW, Pierson JT, *et al*., 2015. Estrogen modulation properties of mangiferin and quercetin and the mangiferin metabolite norathyriol. Food & Function 6(6):1847-1854.

Xu J, Hu HK, Jiang HX, *et al*., 2025. The therapeutic mechanisms of quercetin on inflammatory diseases: An update. Inflammopharmacology 33(6):3015-3049.

Yamamoto K, Takahara K, Oyadomari S, *et al*., 2010. Induction of liver steatosis and lipid droplet formation in ATF6α-knockout mice burdened with pharmacological endoplasmic reticulum stress. Molecular Biology of the Cell 21(17):2975-2986.

Yan Q, Li CY, Li JF, *et al*., 2024. Protective effects of isostrictiniin against high-fat, high-sugar diet-induced steatosis in MASLD mice via regulation of the AMPK/SREBP-1c/ACC pathway. Nutrients 16(22):3876.

Yang H, Yang TT, Heng C, *et al*., 2019. Quercetin improves nonalcoholic fatty liver by ameliorating inflammation, oxidative stress, and lipid metabolism in db/db mice. Phytotherapy Research 33(12):3140-3152.

Zou Y, Zhong L, Hu C, *et al*., 2020. Association between the alanine aminotransferase/aspartate aminotransferase ratio and new-onset non-alcoholic fatty liver disease in a nonobese Chinese population: A population-based longitudinal study. Lipids in Health and Disease 19(1):245.